

# Modified Drug Release from SiO<sub>2</sub>/Polyhydroxybutyrate Composite Prepared Using Bamboo Leaf-Derived Silica

Enobong R. ESSIEN\*<sup>o</sup>

**Modified Drug Release from SiO<sub>2</sub>/Polyhydroxybutyrate Composite Prepared Using Bamboo Leaf-Derived Silica**

## SUMMARY

The ability of a controlled or modified drug delivery system to supply the drug in a sustained way and assure on-demand bioavailability makes it preferable to traditional drug administration. Due to the reliance on alkoxysilane silica precursors, the preparation of silical polymer composite delivery material is costly. As a result, this study looked into using the bamboo leaf as a silica starting material. To evaluate in vitro degradability and modified-release in phosphate-buffered saline (PBS) solution, the ash from the bamboo leaf was mixed with polyhydroxy butyrate (PHB) solution to make a (SiO<sub>2</sub>/PHB) composite, which was then loaded with the medication, tetracycline hydrochloride (TCH). The shape, phase composition, and chemical bond characteristics of the materials were evaluated using scanning electron microscopy (SEM), X-ray diffractometry (XRD), and Fourier transform infrared spectroscopy. An ultraviolet (UV) spectrophotometer was used to determine the TCH release profile. The SiO<sub>2</sub>/PHB composite was found to have a successful drug loading ability. In addition to regulated degradability in PBS, the composite exhibited a steady and sustained TCH release, with the degradation solution pH remaining below safe limits. As a result, the formulation of SiO<sub>2</sub>/PHB for continuous TCH delivery from bamboo leaf-derived silica suggests a significant potential economic benefit for a safe, regulated drug delivery method.

**Key Words:** Bamboo leaf, alkoxysilanes, composites, modified drug release, silica, tetracycline hydrochloride.

**Bambu Yaprağından Elde Edilen Silika Kullanılarak Hazırlanan SiO<sub>2</sub>/Polihidroksibütirat Kompozitten Modifiye İlaç Salımı**

## ÖZ

Kontrollü veya modifiye edilmiş ilaç salım sistemleri, ilacı sürekli vermesi ve istenilen biyoyararlanımı sağlaması nedeniyle konvansiyonel ilaç uygulama sistemlerine göre tercih edilmektedirler. Alkoksisilan silika prekürsörlerine bağlı olarak silika/polimer kompozitlerin taşıyıcı malzeme olarak üretilmeleri pahalıdır. Sonuç olarak, bu çalışma bambu yaprağını silika başlangıç malzemesi olarak kullanmayı amaçlamıştır. İn vitro bozunmayı ve modifiye edilmiş salımı fosfat tamponlu tuz çözeltisinde (PBS) değerlendirmek için, tetrasiklin hidroklorür (TCH) ile yüklenen bir (SiO<sub>2</sub>/PHB) kompozit yapmak için bambu yaprağından gelen kül, polihidroksibütirat (PHB) çözeltisi ile karıştırılmıştır. Malzemelerin şekli, faz bileşimi ve kimyasal bağ özellikleri, taramalı elektron mikroskobu (SEM), X-ışını difraktometrisi (XRD) ve Fourier dönüşümü kızılötesi spektroskopisi kullanılarak değerlendirildi. TCH salınım profilini belirlemek için bir ultraviyole (UV) spektrofotometre kullanıldı. SiO<sub>2</sub>/PHB kompozitinin başarılı bir ilaç yükleme yeteneğine sahip olduğu bulundu. İlave olarak PBS'de düzenlenmiş bozunabilirliğe ek olarak, kompozitin, bozunma çözeltisi pH'nın güvenli sınırların altında kalmasıyla, TCH'yi sabit ve sürekli bir şekilde saldığı bulundu. Sonuç olarak, bambu yaprağından türetilen silikadan sürekli TCH salımı için SiO<sub>2</sub>/PHB formülasyonu, güvenli, düzenlenmiş bir ilaç verme yöntemi olarak önemli bir potansiyel ekonomik fayda sağlayacaktır.

**Anahtar Kelimeler:** Bambu yaprağı, Alkoksisilan, kompozitler, modifiye edilmiş ilaç salımı, silika, tetrasiklin hidroklorür.

Received: 14.06.2021

Revised: 18.09.2021

Accepted: 22.11.2021

\* ORCID: 0000-0002-0010-5721 Department of Chemical and Food Sciences, Bells University of Technology, P.M.B 1015 Ota, Ogun State, Nigeria

<sup>o</sup> Corresponding Author; Enobong R. ESSIEN

Phone: +234-8139447446, e-mail: reggiessen@gmail.com

## INTRODUCTION

The purpose of targeted drug delivery systems is to deliver medications at the right dosage for the right amount of time to a specific site of action in the body. This is done to ensure that the medicine has the required pharmacological effect while avoiding any negative effects on other organs or tissues. For successful therapy, controlled drug delivery systems (DDS) attempt to achieve efficient drug administration while avoiding systemic and/or local side effects (Anselmo and Mitragotri, 2014). DDS has several advantages over traditional drug administration, including enhanced efficacy, lower toxicity, and improved tissue or cell targeting (Uhrich, 1999). Other benefits include reduced administration frequency, improved patient compliance, and higher commercial worth of marketed medications due to patent extension.

Many scientists have concentrated their efforts on biodegradable polymers and how to modify their properties in the previous decade. Based on this, combining inorganic and organic nanomaterials has proven to be a more persuasive way for generating nanocomposites with biodegradable polymers as the organic component. When compared to neat polymers, nanocomposites with superior melt strength, mechanical properties, crystallization rate, barrier characteristics, thermal stability, and degradation rate, can overcome the problem of drug burst.

Because of their ability to create porous architecture, uniform distribution of guest molecules in porous space, surface charge management, free dispersion throughout the body, and, most importantly, their size, optical characteristics, high surface area, low density, adsorption capacity, and encapsulation ability, porous silica particles (PSP) are appealing in drug delivery (Sakai-Kato, 2011; Bitar, 2012). As a result, PSP, especially in the form of mesoporous silica nanoparticles (MSN) is at the forefront of drug delivery. According to *in vitro* and *in vivo* biocompatibility tests (Fruijtier-Poelloth, 2012; Kettiger, 2015), PSP is

also safe and well-tolerated.

The traditional routes to PSP are alkoxysilanes (Parfenyuk and Dolinina, 2014; Mohseni, 2015; Parfenyuk and Dolinina, 2017; Kierys, 2020). However, the toxicity of alkoxysilanes is well documented (Nakashima, 1998), and besides, their high cost (Essien, 2012) renders them unattractive for large-scale synthesis of PSP. Before reaching the market, place nanomedicines are expected to satisfy the core objectives of clinical translation and industrial technology transfer. The latter would involve the scaling-up process (Shi, 2016), where reproducibility and the total costs are likely to constitute obstacles for effective commercialization.

A positive alternative could be based on a change of strategy towards biomass-derived silica. The advantage is not limited to eco-friendliness but renewability and cost-effectiveness. The advantages are even more profound if the biomass does not serve as a food resource or has little or no significant pharmacological or industrial applications.

The bamboo leaf is one important biomass that has the potential to meet these requirements. It is regarded as waste or garbage and, consequently, has received little attention in the past. Nonetheless, there are studies (Dwivedi, 2011; Mohapatra, 2011; Aminullah, 2015) showing that the SiO<sub>2</sub> content of bamboo ranges from 65.85 – 82.86%. The current study, therefore, explored the use of silica extracted from the bamboo leaf for the preparation of a carrier system for modified drug release. Based on literature information, no previous research has been done on the creation of a silica-based polymer composite for modified drug release using bamboo leaf silica.

## MATERIALS AND METHODS

### Materials

The silica precursor, bamboo (*Bambusa vulgaris*) leaves were collected in a bush around the University of Lagos, Lagos, South-West, Nigeria, and authenticat-

ed at the University of Lagos Herbarium (LUH5493). The following analytical grade reagents were purchased from Sigma-Aldrich: Poly(3-hydroxybutyrate) (PHB), (96% purity with average molecular weight = 600,000 g/mol) and chloroform (HPLC grade, assay 99%); doubly-distilled deionised water, sodium chloride, sodium dihydrogen phosphate, potassium chloride, and disodium hydrogen phosphate were used for phosphate-buffered saline solution preparation (pH 7.4). Tetracycline hydrochloride (TCH) (capsules, 500 mg) was purchased from a registered pharmacy.

#### **Silica Preparation**

Biosilica was extracted from the bamboo leaves as described previously by Kow et al. (2014). The leaves were initially separated from sand, stone, and other unwanted materials, then washed with double distilled deionized water before sun-drying. The leaves were further dried in a hot air oven at 105 °C for 72 hours and ground to form a powder. The pulverised material was transferred into a muffle furnace and burnt at 800 °C for 3 hours at a ramping rate of 10 °C/min to obtain silica ash.

#### **Preparation of SiO<sub>2</sub>/PHB Composite**

The SiO<sub>2</sub>/PHB composite was prepared by the nanoprecipitation technique. Accordingly, 1 g of the biosilica was initially dispersed in chloroform (30 mL) with an ultra-sonicated (Ultrasonic cleaner, CLEAN 120HD) at 40 W, 30 °C for 5 min. Afterwards, PHB powder (0.5 g) was added and the temperature was adjusted to 45 °C. Next, the mixture was sonicated further for 2 hours to complete the dissolution of the PHB to form a colloidal solution. On completion, the mixture was immediately cast into cylindrical moulds measuring 10.4 mm × 5.2 mm (height x diameter) in dimension and allowed to dry at ambient conditions for 7 days. After removal from the mould, the sample was labelled SPC.

#### **Preparation of SiO<sub>2</sub>/PHB-TCH Composite**

The biosilica was similarly dispersed in chloroform to the neat silica/PHB composite to perform the TCH

drug loading of the silica/PHB composite. Thus, after sonicating the biosilica for 5 min, PHB powder (0.5 g) was added and sonicated further for 2 min, then 150 mg of the model drug, TCH (corresponding to 10 wt% of matrix weight) was dispersed in the polymer matrix. This resulting suspension was again sonicated at 45 °C for 2 h. Then, the homogeneous solution obtained was cast into cylindrical moulds measuring 10.4 mm × 5.2 mm (height x diameter) in dimension and allowed to dry the room temperature for 7 days. Upon completion of the drying process and removal from the mould, the sample was tagged SPC/TCH.

#### **Characterization**

The tensile and compressive strengths of the drug-loaded and unload composites were measured on a universal testing machine (MODEL BAB-200, Transcell Technology) with a 100 kgf load, at a cross-head rate of 50 mm/min. The samples presented for the tests were in triplicates.

In an energy dispersive X-ray fluorescence (EDXRF) spectrometer, elemental analysis was conducted to determine the composition of the samples (Minipal 4). The samples were pulverized into extremely fine particles and homogeneously sieved through a 150-micron mesh sieve. On the machine's sample changer, the appropriate masses of the samples were weighed into sample cups. For oxides, the voltage was set at 14 kV using a Kapton filter, and for trace elements, it was adjusted to 20 kV with an Ag/Al-thin filter.

A scanning electron microscope was used to examine the microstructure of the composites (Phenom ProX, Phenomworld). Using a quorum-Q150R Plus E sputter coater, the samples were distributed over carbon conductive tape and sputter-coated with 5 nm gold.

The phase composition and crystallinity of the materials were investigated using an X-ray diffractometry (XRD) (Empyrean Panalytical) system that used Cu K radiation with a wavelength of 1.5418 nm

and a tube current of 40 mA to generate the X-ray. The samples were evaluated using the  $\theta$  parameters on the reflection-transmission spinner stage. With a 2 step of 0.026261 at 8.67 seconds each step, the diffraction angle was scanned from 4 to 75°.

The spectra depicting the chemical bond properties of the composites were obtained from a Fourier transform infrared spectrometer (Agilent Technology Cary 630 FTIR) in transmittance mode. The spectra were obtained by averaging 30 scans at 8 cm<sup>-1</sup> resolutions over the spectral scan range of 4000– 650 cm<sup>-1</sup>.

#### Experiment on Drug Release *In Vitro*

For the *in vitro* drug release study, the SPC/TCH composite (0.25 g) was immersed in a 100 mL release medium of PBS, pH 7.4 in a clear glass vial and incubated at 37 °C with constant agitation of 50 rpm for a maximum of 28 days. The PBS solution was withdrawn at pre-defined time intervals to determine the quantity of TCH released, which was measured as absorbance with a UV/visible spectrophotometer (T70+ UV/Vis Spectrometer, PG Instruments Ltd.) at a wavelength of 358 nm. The TCH stock concentration of 5–100 µg/mL in PBS solution was first used to obtain the calibration curve, and the drug concentration was extrapolated from an absorbance-concentration calibration curve. The quantity of the cumulative TCH released from the SPC/TCH composite was plotted against time and calculated relative to the initial drug weight in the polymer matrix. The drug release evaluation was carried out in triplicates.

#### *In Vitro* Degradation Test

The weight loss of the SPC/TCH composite was studied for a maximum of 28 days by incubating 0.39 g of the sample in 20 mL of PBS (pH 7.4) at 37 °C with constant stirring at 50 rpm. The samples were stored in glass vials secured with a lid to prevent evaporation of the PBS buffer. The PBS soaking medium was

not refreshed during the incubation period (1, 7, 14, 21, and 28 days) to allow for the daily (1 – 14 days) determination of pH changes. The change in pH of the degradation media was monitored with a pH meter (Metrohm, Germany), while the test environment was UV-sterilised to prevent microbial contamination, which could affect the validity of the result. After removing from PBS, the samples were cleaned with distilled-deionized water and dried in the oven at 105 °C until a constant weight was obtained, then cooled and stored in a desiccator at ambient temperature for 60 min. The degradation (weight loss) in percentage was estimated according to the relation (1) (Yu, 2013)  $W_0$  and  $W_t$  are the dry weights of the original and degraded specimens, respectively, and  $D$  is the degradation rate.

$$D = [(W_0 - W_t)/W_0] \times 100\% \quad (1)$$

## RESULTS AND DISCUSSION

### Composition of the Bamboo Leaf-Derived Silica

The yield of the silica based on the dry weight of the bamboo leaf biomass was 46.27%. This result compares with the study of Rangaraj and Venkatachalam (2017) which obtained 49.88% of silica from bamboo leaf biomass after burning dried bamboo leaf at 750 °C for 3 h in a muffle furnace. The elemental composition of the calcined bamboo leaves as determined by EDXRF is given in Figure 1. The analysis shows a high percentage abundance of silicon (80%), which agrees with previous reports (Arumugam, 2018; Renita, 2019) and hence indicates that bamboo leaf is a rich source of silica. Traces of calcium, phosphorus, potassium, aluminium, magnesium, sulphur, and chlorine were also observed. It is very interesting to observe the absence of toxic heavy metals, like Pb, As, and Ni, indicating that the prepared biosilica is safe for use in preparing drug delivery vehicles.

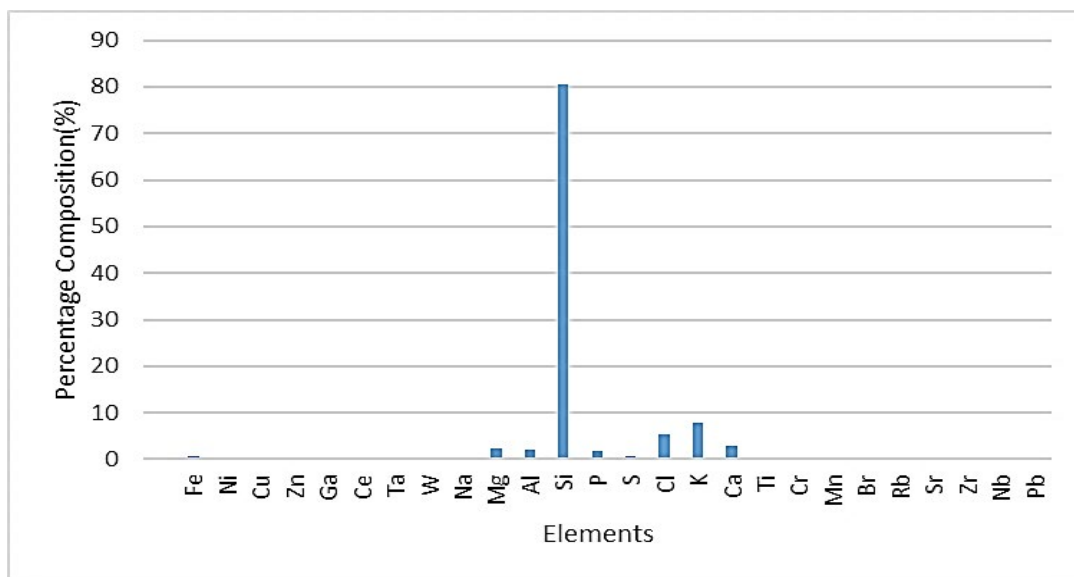


**Figure 1.** EDXRF spectrum of the bamboo leaf-derived silica showing a high percentage content of Si and the absence of toxic heavy metals.

**Mechanical Properties**

The compressive strength for SPC was  $0.897 \pm 0.12$  MPa, while the tensile strength gave  $6.222 \pm 0.24$  MPa and a force downfield of 8.952 Kgf. From the comparison of typical composite scaffold stress-strain curves, this moderate result was due to the presence of pores in the microstructure caused by incorporation of silica into the material. The result shows that the material was not compact but contained pore structures that could enable the encapsulation of drugs if applied in controlled/modified release. The compressive strength of SPC/TCH was  $0.989 \pm 0.3$  MPa, while the tensile strength gave  $6.884 \pm 0.27$  MPa and with a force downfield of 8.952 Kgf. The slight difference in the strength of the drug-loaded and unloaded composites was due to the filling of the pores in the composite by the drug. This result compares to a previous study (Chou and Woodrow, 2017) on drug release from electrospun fibres of polycaprolactone (PCL) and poly(D, L-lactic-co-glycolic) acid (PLGA) blends. The fibres in this investigation, which had a tensile strength of up to 6.409 MPa, declined dramati-

cally in PBS; 20% after 1 h, 30% after 48 hours, and 90% after 240 hours in the release media. After 1 h, the average tensile strength of the drug-loaded fibres had decreased by 60%, 50%, and 50%, respectively, and after 240 hours, the tensile strength reduced by 80%, indicating that drug release leads to a decrease in mechanical properties.

**Morphology**

The microstructure of SPC (Figure 2(a)) revealed the presence of aggregates of SiO<sub>2</sub> crystals embedded in the polymer matrix. These sites are seen all over the surface of the polymer matrix. The surface on which the particles are embedded appear flat and broad, thus presenting a large surface area. A large surface area is important to confer a high specific capacity needed to provide high drug loading capacity (Pang and Nazar, 2016). After loading with TCH (Figure 2(b)), the surface became more compact with a larger number of particle aggregates, increased in the number of embedment sites, and consequently, giving a much larger surface area. This is caused by the drug molecules filling up the micropores in the material.

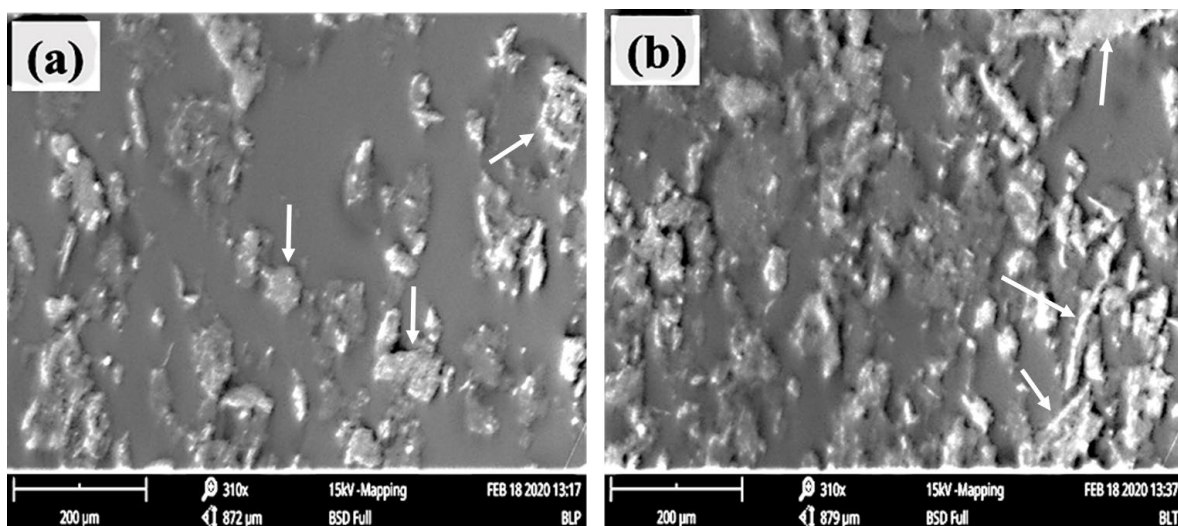


**Figure 2.** SEM micrographs of (a) SPC showing SiO<sub>2</sub> embedded in PHB matrix and (b) SPC/TCH; where SiO<sub>2</sub> and TCH are embedded in the PHB matrix. White arrows show some embedment sites.

### Diffraction Patterns

The diffractograms showing the phase identification of the crystallographic structure of the composites are presented in Figure 3. The diffraction pattern of SPC exhibited peaks that match both PHB and SiO<sub>2</sub> components in the sample (Figure 3(a)). Prominent peaks are observed at  $2\theta$  21.5°, 26.5°, 28.5°, 31.5°, 36.5°, and 40°  $2\theta$  which match cristobalite (SiO<sub>2</sub>) in both angular position and intensity when indexed with the standard reference file ICDD # -01-077-1317 (Hao, 2015). The peaks corresponding to PHB are located at  $2\theta$  13.5°, 17.0°, 45°, and 57° (Renita, 2019). The SPC sample exhibited a semi-crystalline behaviour, judging from the sharpness and intensity of diffraction peaks and the nature of their pattern at the baseline. The presence of SiO<sub>2</sub> and PHB peaks in the XRD spectrum support the SEM result, which showed SiO<sub>2</sub> embedment in a polymer matrix.

The XRD pattern after drug loading (SPC/TCH) is depicted in Figure 3(b). All the SiO<sub>2</sub> and PHB peaks identified in the spectrum of SPC are still present. In addition, three new peaks emerged at the angular positions  $2\theta$  10.55°, 26.18°, and 30.95°, corresponding to the TCH crystal plane reflections (Thangadurai,

2005; Blanchard, 1989). There was no difference in diffraction patterns between the SPC and SPC/TCH. However, a slight decrease in baseline intensity was observed for SPC/TCH. This is attributed to the impregnation of the drug into the polymer matrix (Basu and Adhiyaman, 2008).

### Bond Properties

The vibrational modes of the sample without the drug (SPC) and that containing the drug (SPC/TCH) are presented in the FTIR spectra (Figure 4). The spectrum of SPC (Figure 4(a)) contains bands at 1738 and 1207 cm<sup>-1</sup> attributed to the vibrational stretching of C=O and C—O bonds, respectively, and are due to the presence of PHB. The presence of PHB in the sample is further indicated by the C—H stretch at 2937 cm<sup>-1</sup>. The successful incorporation of silica into the polymer matrix is confirmed by the peaks observed at 1114, 1051, 988, 908, and 855 cm<sup>-1</sup>. The peaks at 1114 and 1051 correspond to Si—O—Si stretching vibrations (asymmetric). The signal at 988 cm<sup>-1</sup> is considered for the asymmetric vibrational stretching of Si—OH, while those at 908 and 855 are ascribed to the stretching (symmetric) of Si—O—Si bond (Liu, 2004).

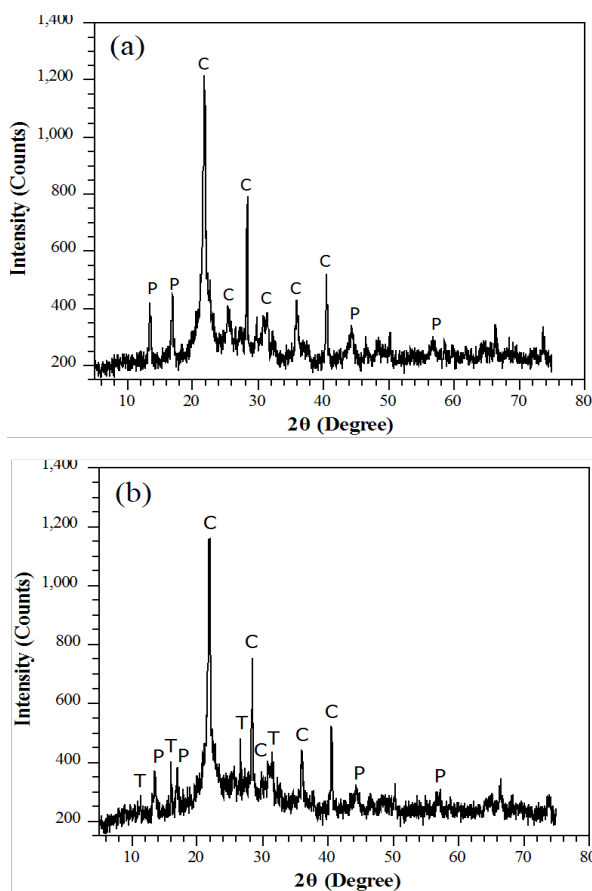


**Figure 3.** XRD patterns of (a) SPC and (b) SPC/TCH. C = cristobalite, P = PHB and T = TCH.

The large peaks at 3587 and 3335  $\text{cm}^{-1}$  are linked to O–H stretching of surface water molecules, as evidenced by the angular vibration at 1628  $\text{cm}^{-1}$  (Adams,

2017). The presence of hydroxyl group (OH) in the sample confirms the hydrophilicity of the silica. The appearance of the hydroxyl group can be attributed to the silanol bonds solely responsible for the adsorptive behaviour of hydrophilic silica and silicate surfaces. These silanol groups can participate in hydrogen bonding between the silica and PHB, resulting in the formation of a rigid material. It is therefore suggested that the semi-crystalline nature of SPC observed in the XRD result was due to this phenomenon.

After drug loading, the sample (SPC/TCH) gave some shifts in vibrational frequencies as observed in Figure 4(b). The C=O and C–O stretching are now observed at 1729 and 1237  $\text{cm}^{-1}$ , respectively, while the C–H stretching bond undergoes vibrational coupling to give two modes: at 2922 and 2855  $\text{cm}^{-1}$  due to the methylene ( $\text{CH}_2$ ) hydrogens of the PHB. Furthermore, the Si–O–Si asymmetric stretching vibration, which was observed in the unloaded sample became diffuse, while the one initially located at 1051  $\text{cm}^{-1}$  is shifted to 1021  $\text{cm}^{-1}$ . Also, the peaks linked to the Si–O–Si vibrational symmetric stretching signal disappeared from the spectrum. These manifestations were a result of the impregnation of the drug into the polymer matrix. It is also worthy of mention that the disappearance of some of the FTIR peaks justify the reduction in the baseline intensity of the XRD peaks observed previously in the SPC/TCH XRD spectrum (Figure 3(b)).

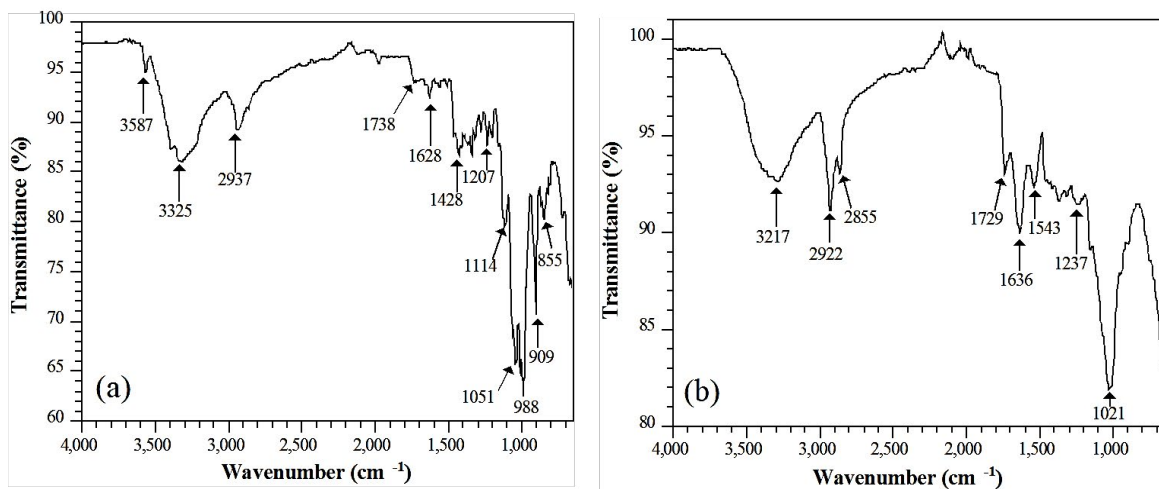


**Figure 4.** The vibrational frequencies and intensities of the bonds present in (a) SPC and (b) SPC/TCH FTIR spectra.

Confirmation of the presence of TCH in the composite was seen by the increase in the intensity of the O–H large band centred at  $3217\text{ cm}^{-1}$ , which was due to the joint contribution of O–H vibrational stretching of the hydroxyl group in surface water and that in the TCH. Additionally, a prominent peak developed at  $1636\text{ cm}^{-1}$  and another smaller one at  $1543\text{ cm}^{-1}$  which is due to C=O stretching in the tetracycline rings (Caminati, 2002).

#### **Biodegradability Assessment of the SiO<sub>2</sub>/PHB-TCH Composite**

The degradation behaviour of SPC/TCH on immersion in PBS solution was monitored for a total duration of 28 days at  $37\text{ }^{\circ}\text{C}$ . The loss of weight and degradability upon immersion were studied using the relation in Equation 1. Figure 5 represents the degradation of the composite at different times after soaking in PBS for 28 days. Degradation was observed to be insignificant at the onset of the study due to a loss of about 6.64% of its initial weight in 24 hours, suggesting slow hydrolytic degradation of the sample. The weight loss increased up to 32% on the 7th day, 58.24% on day 14, 66.50% on the 21st day, and reaching 68.51% loss on the 28th day. The degradation results suggest that most of the components were lost in 28 days after soaking in PBS.

Freier et al. (2002) reported that PHB scaffold gave slow hydrolytic erosion in PBS medium when incubated at  $37^{\circ}\text{C}$  owing to the crystalline and water-resistance nature of PHB. The degradation behaviour often depends on the structure and arrangement of the polymer matrix, pore sizes, and degradation media. The depletion of PHB in the degradation medium by hydrolysis was caused by irregular cleavage of the ester linkages in the polymer matrix, causing a lowering of the molar mass; the reduction in the molar mass results

in loss of weight and macroscopic shapes (Peña, 2006). PHB degradation occurs through hydrolysis and produces butyric acid, which decreased the pH of the PBS solution. The degradation kinetics exhibited by the composite is significant for sustained drug release.

The pH changes of SPC/TCH monitored for 14 days in PHB are depicted in Figure 6. The pH decreased linearly during the first 6 days, then slowed between 6 – 12 days, and remained constant after the 12th day at a value of 7.11. The generation of somewhat acidic breakdown products from the breaking of the ester links in the PHB caused the pH to drop. Interestingly, the pH changes of the medium were at values that would not be cytotoxic such that may lead to aseptic inflammation (Wang, 2016) if the composite material is to serve as an *in vivo* drug delivery vehicle.

#### ***In Vitro* Drug Release Examination**

The release profile of SPC/TCH in the PBS medium at pH 7.4 and at  $37\text{ }^{\circ}\text{C}$  as determined by UV-visible spectroscopy at 358 nm is presented in Figure 7. The TCH cumulative release curves exhibited efficiently sustainable release, giving only a slight biphasic pattern (Figure 7 inset) usually associated with a drug embedded in a polymer as the only encapsulating material (Swornakumari, 2018). A release of  $7.132\text{ }\mu\text{g/mL}$  at 0 - 1 h was observed, which was 4.74 % of the total concentration of the encapsulated drug. After 2 h, the cumulative release was  $9.63\text{ }\mu\text{g/mL}$ ,  $14.60\text{ }\mu\text{g/mL}$  after 1 day, representing 6.40 and 9.70%, respectively. The modified release was sustained beyond these periods until the 28th day. As seen in Figure 7, the cumulative releases were 38.6, 60.89 and 74.5% for 7, 14, and 21 days, respectively. At the end of the 28th day, the cumulative release reached a peak value of  $126.39\text{ }\mu\text{g/mL}$ , accounting for 84% of the drug.

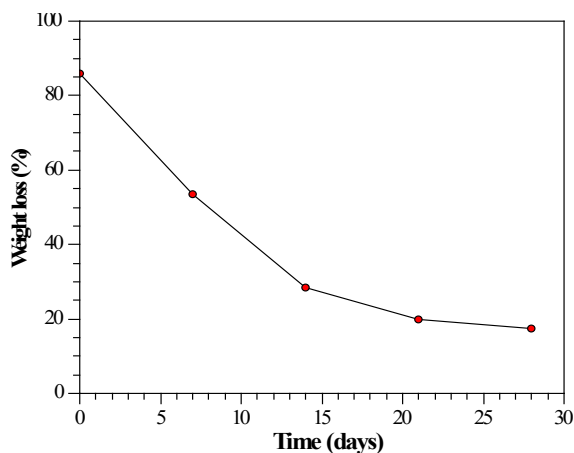


**Figure 5.** *In vitro* degradation (weight loss) of SPC/TCH soaked in PBS for 28 days.

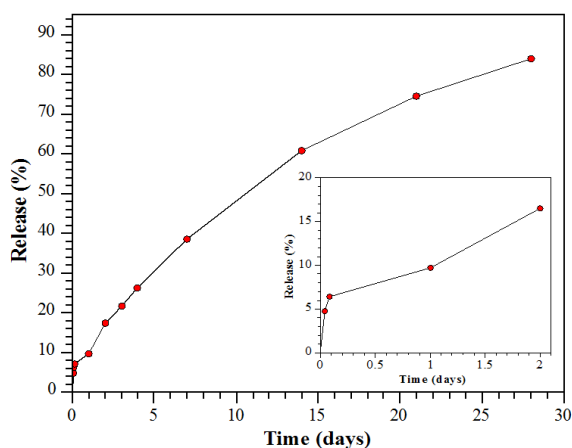


**Figure 7.** *In vitro* TCH release profile of SPC/TCH immersed in PBS for 28 days. The release profile for the first 2 days is shown in the inset.

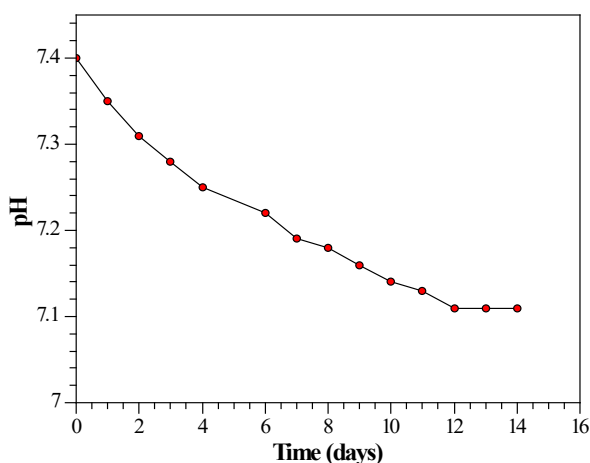
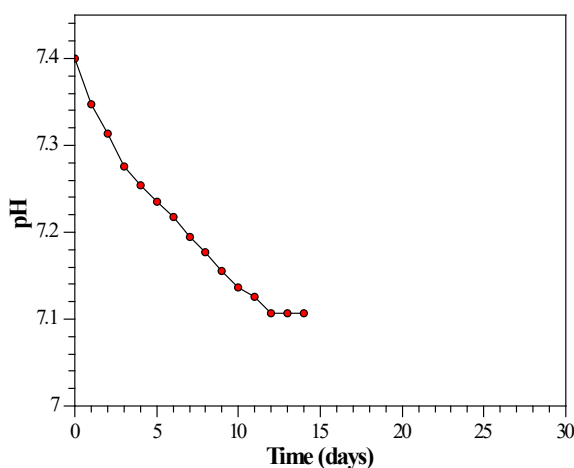


**Figure 6.** pH changes of the SPC/TCH soaked in PBS for 14 days.

The modified release profile can be explained in terms of adsorption of the TCH onto the SiO<sub>2</sub> network structure, which reduced the instantaneous burst release of TCH at the initial stages, thus giving rise to a slow and sustained TCH release. The slight burst of the drug observed during the first 2 hours (Figure 7 inset) was due to incomplete adsorption of the TCH by SiO<sub>2</sub>. Further TCH release was due to bulk diffusion from the silica network structure. The mechanism of drug release from polymeric nanocomposites is usually such that the drug is desorbed from the surface of the nanoparticles and diffused through the pores of the drug vehicle; the polymeric carrier is eroded and degraded as it absorbs water from the release medium. The rate of dissolution is slower for the particles remotely inside the polymeric matrix and often relies on diffusion through the matrix (Fernández-Colino, 2016). Since the core to the surface diffusion rate decreases with time, the rate of release of the drug also decreases, hence, the drug is sustained. The result obtained from this study conforms to an earlier study by Luo et al. (2018), even though they used TiO<sub>2</sub> in place of SiO<sub>2</sub>.

## CONCLUSION

A silica/PHB composite was prepared where the silica was obtained economically from a bamboo leaf. The composite material was loaded with the drug TCH to serve as a drug carrier system to study modified drug release. Results obtained indicated a successful encapsulation of the TCH into the polymer matrix. The drug release test conducted on the material gave a good sustained release profile where the SiO<sub>2</sub> component played a significant role in adsorbing the TCH molecule, thus leading to its delayed release. The degradation rate of the composite during a 28-day duration in PBS showed the ability of the PHB-silicate network to degrade controllably while releasing the drug, which is optimal for a material intending to serve as an *in vivo* drug release vehicle.

Of great significance is that the silica was obtained from biomass, which besides being an inexpensive source, the preparation process poses no health concerns or danger to the environment when compared to the corresponding analytical grade silica starting materials, usually alkoxysilanes. Also worthy of note is that the bamboo plant is widely available and, in most places, where it grows, it serves as a biowaste, thus making it attractive as large-scale silica starting material for preparing SiO<sub>2</sub>/polymer composite for drug delivery application.

## CONFLICT OF INTEREST

All the authors of this article declared no conflict of interest.

## AUTHOR CONTRIBUTION STATEMENT

Initial literature survey, experimental design, sourcing for materials, laboratory work, data acquisition and analysis, interpretation of result, writing and revision of the manuscript (Essien, E.R.).

## ACKNOWLEDGEMENTS

The author is appreciative to Bells University of Technology, Ota's Central Teaching and Research

Laboratory (CTRL) for allowing them to conduct this research.

## REFERENCES

- Adams, L. A., Essien, E. R., Adesalu, A. T., & Julius, M. L. (2017). Bioactive glass 45S5 from diatom bi-silica. *Journal of Science: Advanced Materials and Devices*, 2(4), 476–482. <https://doi.org/10.1016/j.jsamd.2017.09.002>
- Aminullah, Rohaeti, E., & Irzaman. (2015). Reduction of high purity silicon from bamboo leaf as basic material in development of sensors manufacture in satellite technology. *Procedia Environmental Sciences*, 24, 308–316. <https://doi.org/10.1016/j.proenv.2015.03.040>
- Anselmo, A. C., & Mitragotri, S. (2014). An overview of clinical and commercial impact of drug delivery systems. *Journal of Controlled Release*, 190, 15–28. <https://doi.org/10.1016/j.jconrel.2014.03.053>
- Arumugam, A., Karuppasamy, G., & Jegadeesan, G. B. (2018). Synthesis of mesoporous materials from bamboo leaf ash and catalytic properties of immobilized lipase for hydrolysis of rubber seed oil. *Materials Letters*, 225, 113–116. <https://doi.org/10.1016/j.matlet.2018.04.122>
- Basu, S., & Adhiyaman, R. (2008). Preparation and Characterization of Nitrendipine-loaded Eudragit RL 100 microspheres prepared by an emulsion-solvent evaporation method. *Tropical Journal of Pharmaceutical Research*, 7(3). <https://doi.org/10.4314/tjpr.v7i3.14688>
- Bitar, A., Ahmad, N. M., Fessi, H., & Elaissari, A. (2012). Silica-based nanoparticles for biomedical applications. *Drug Discovery Today*, 17(19–20), 1147–1154. <https://doi.org/10.1016/j.drudis.2012.06.014>
- Blanchard, F. N. (1989). The space group and reference powder diffraction data for tetracycline hydrochloride, C<sub>22</sub>H<sub>24</sub>N<sub>2</sub>O<sub>8</sub>HCl. *Powder Diffraction*, 4(2), 103–105.

- Caminati, G., Focardi, C., Gabrielli, G., Gambinosi, F., Mecheri, B., Nocentini, M., & Puggelli, M. (2002). Spectroscopic investigation of tetracycline interaction with phospholipid Langmuir-Blodgett films. *Materials Science and Engineering: C*, 22(2), 301–305. [https://doi.org/10.1016/s0928-4931\(02\)00217-5](https://doi.org/10.1016/s0928-4931(02)00217-5)
- Chou, S. F., & Woodrow, K. A. (2017). Relationships between mechanical properties and drug release from electrospun fibers of PCL and PLGA blends. *Journal of the Mechanical Behavior of Biomedical Materials*, 65, 724–733. <https://doi.org/10.1016/j.jmbbm.2016.09.004>
- Dwivedi, V. N., Singh, N. P., Das, S. S., & Singh, N. B. (2006). A new pozzolanic material for cement industry: bamboo leaf ash. *International Journal Physical Sciences*, 1(3), 106–111.
- Essien, E. R., Adams, L. A., Shaibu, R. O., Olasupo, I. A., & Oki, A. (2012). Economic route to sodium-containing silicate bioactive glass scaffold. *Open Journal of Regenerative Medicine*, 01(03), 33–40. <https://doi.org/10.4236/ojrm.2012.13006>
- Fernández-Colino, A., Bermudez, J., Arias, F., Quinteros, D., & Gonzo, E. (2016). Development of a mechanism and an accurate and simple mathematical model for the description of drug release: Application to a relevant example of acetazolamide-controlled release from a bio-inspired elastin-based hydrogel. *Materials Science and Engineering: C*, 61, 286–292. <https://doi.org/10.1016/j.msec.2015.12.050>
- Freier, T., Kunze, C., Nischan, C., Kramer, S., Sternberg, K., Saß, M., . . . Schmitz, K. P. (2002). *In vitro* and *in vivo* degradation studies for development of a biodegradable patch based on poly(3-hydroxybutyrate). *Biomaterials*, 23(13), 2649–2657. [https://doi.org/10.1016/s0142-9612\(01\)00405-7](https://doi.org/10.1016/s0142-9612(01)00405-7)
- Fruijtier-Poelloth, C. (2012). The toxicological mode of action and the safety of synthetic amorphous silica - A nanostructured material. *Toxicology*, 294(2-3), 61–79. <https://doi.org/10.1016/j.tox.2012.02.001>
- Hao, R., Yan, Z., Huamin, Z., Jinxiang, C. (2015). Production and evaluation of biodegradable composites based on polyhydroxybutyrate and polylactic Acid reinforced with short and long pulp fibers. *Cellulose Chemical Technology*, 49(7-8), 641–652.
- Kettiger, H., Sen Karaman, D., Schiesser, L., Rosenholm, J. M., & Huwyler, J. (2015). Comparative safety evaluation of silica-based particles. *Toxicology in Vitro*, 30(1), 355–363. <https://doi.org/10.1016/j.tiv.2015.09.030>
- Kierys, A., Zaleski, R., Grochowicz, M., Gorgol, M., & Sienkiewicz, A. (2020). Polymer-mesoporous silica composites for drug release systems. *Microporous and Mesoporous Materials*, 294, 109881. <https://doi.org/10.1016/j.micromeso.2019.109881>
- Liu, X., Ding, C., & Chu, P. K. (2004). Mechanism of apatite formation on wollastonite coatings in simulated body fluids. *Biomaterials*, 25(10), 1755–1761. <https://doi.org/10.1016/j.biomaterials.2003.08.024>
- Luo, W., Geng, Z., Li, Z., Wu, S., Cui, Z., Zhu, S., . . . Yang, X. (2018). Controlled and sustained drug release performance of calcium sulfate cement porous TiO<sub>2</sub> microsphere composites. *International Journal of Nanomedicine, Volume 13*, 7491–7501. <https://doi.org/10.2147/ijn.s177784>
- Mohapatra, S., Sakthivel, R., Roy, G. S., Varma, S., Singh, S. K., & Mishra, D. K. (2011). Synthesis of β-SiC powder from bamboo leaf in a DC extended thermal plasma reactor. *Materials and Manufacturing Processes*, 26(11), 1362–1368. <https://doi.org/10.1080/10426914.2011.557127>
- Mohseni, M., Gilani, K., & Mortazavi, SA. (2015). Preparation and characterization of Rifampin loaded mesoporous silica nanoparticles as a potential system for pulmonary drug delivery. *Iranian Journal Pharmaceutical Research*, 14(1), 27–34. PMID: 25561909; PMCID: PMC4277616.
- Nakashima, H., Omae, K., Takebayashi, T., Ishizuka, C., & Uemura, T. (1998). Toxicity of silicon compounds in semiconductor industries. *Journal of Occupational Health*, 40(4), 270–275. <https://doi.org/10.1539/joh.40.270>

- Pang, Q., & Nazar, L. F. (2016). Long-life and high-area-capacity Li-S batteries enabled by a lightweight polar host with intrinsic polysulfide adsorption. *ACS Nano*, *10*(4), 4111–4118. <https://doi.org/10.1021/acsnano.5b07347>
- Parfenyuk, E. V., & Dolinina, E. S. (2014). Design of silica carrier for controlled release of molsidomine: Effect of preparation methods of silica matrixes and their composites with molsidomine on the drug release kinetics *in vitro*. *European Journal of Pharmaceutics and Biopharmaceutics*, *88*(3), 1038–1045. <https://doi.org/10.1016/j.ejpb.2014.09.007>
- Parfenyuk, E. V., & Dolinina, E. S. (2017). Development of novel warfarin-silica composite for controlled drug release. *Pharmaceutical Research*, *34*(4), 825–835. <https://doi.org/10.1007/s11095-017-2111-9>
- Peña, J., Corrales, T., Izquierdo-Barba, I., Doadrio, A. L., & Vallet-Regí, M. (2006). Long term degradation of poly( $\epsilon$ -caprolactone) films in biologically related fluids. *Polymer Degradation and Stability*, *91*(7), 1424–1432. <https://doi.org/10.1016/j.polymdegradstab.2005.10.016>
- Ranjaraj, S., & Venkatachalam, R. (2017). A lucrative chemical processing of bamboo leaf biomass to synthesize biocompatible amorphous silica nanoparticles of biomedical importance. *Applied Nanoscience*, *7*, 145–153. <https://doi.org/10.1007/s13204-017-0557-z>
- Ren, H., Zhang Y., Zhai, H., & Chen, J. (2015). Production and evaluation of biodegradable composites based on polyhydroxybutyrate and polylactic acid reinforced with short and long pulp fibers. *Cellulose Chemical Technology*, *49*(7-8), 641–652.
- Renita, M, Halimatussa'diah, S, Ruri, R., & Syahputri, Z. (2019). Synthesis and characterization of K-silica catalyst based bamboo-leaves for transesterification reaction. *AIP Conference Proceeding*, *2085*, 020069. <https://doi.org/10.1063/1.5095047>
- Sakai-Kato, K., Hasegawa, T., Takaoka, A., Kato, M., Toyooka, T., Utsunomiya-Tate, N., & Kawanishi, T. (2011). Controlled structure and properties of silicate nanoparticle networks for incorporation of biosystem components. *Nanotechnology*, *22*(20), 205702. <https://doi.org/10.1088/0957-4484/22/20/205702>
- Shi, J., Kantoff, P. W., Wooster, R., & Farokhzad, O. C. (2016). Cancer nanomedicine: progress, challenges and opportunities. *Nature Reviews Cancer*, *17*(1), 20–37. <https://doi.org/10.1038/nrc.2016.108>
- Swornakumari, C., Meignanalakshmi, S., Legadevi, R., & Palanisammi, A. (2018). Preparation of microspheres using poly-3-hydroxybutyrate biopolymer and its characterization. *Journal of Environmental Biology*, *39*(3), 331–338. <https://doi.org/10.22438/jeb/39/3/MRN-315>
- Thangadurai, S., Abraham, J. T., Srivastava, A. K., Nataraja Moorthy, M., Shukla, S. K., & Anjaneyulu, Y. (2005). X-Ray Powder Diffraction Patterns for Certain BETA.-Lactam, Tetracycline and Macrolide Antibiotic Drugs. *Analytical Sciences*, *21*(7), 833–838. <https://doi.org/10.2116/analsci.21.833>
- Uhrich, K. E., Cannizzaro, S. M., Langer, R. S., & Shakesheff, K. M. (1999). Polymeric systems for controlled drug release. *Chemical Reviews*, *99*(11), 3181–3198. <https://doi.org/10.1021/cr940351u>
- Wang, S., Liu, F., Zeng, Z., Yang, H., & Jiang, H. (2015). The protective effect of bafilomycin A1 against cobalt nanoparticle-induced cytotoxicity and aseptic inflammation in macrophages *in vitro*. *Biological Trace Element Research*, *169*(1), 94–105. <https://doi.org/10.1007/s12011-015-0381-9>
- Yu, L., Li, Y., Zhao, K., Tang, Y., Cheng, Z., Chen, J., . . . Wu, Z. (2013). A novel injectable calcium phosphate cement-bioactive glass composite for bone regeneration. *PLoS ONE*, *8*(4), e62570. <https://doi.org/10.1371/journal.pone.0062570>